the Graduate School of the University of Wisconsin, and a fellowship (T.P.L.) provided by the Dozart Fund of the Analytical Division of the American Chemical Society (Professor F. A. Guthrie, sponsor).

Registry No. Polystyrene (homopolymer), 9003-53-6; poly(α-methylstyrene) (homopolymer), 25014-31-7; tetrachlorobisphenol A polycarbonate (SRU), 26913-25-7; (carbonic acid)·(tetrachlorobisphenol A) (copolymer), 26814-08-4.

References and Notes

(1) Thurston, G. B.; Schrag, J. L. *J. Chem. Phys.* **1966**, *45*, 3373.
(2) Thurston, G. B. *J. Chem. Phys.* **1967**, *47*, 3582.
(3) Thurston, G. B.; Schrag, J. L. *J. Polym. Sci., Part A-2* **1968**, *6*, 1331.
(4) Thurston, G. B.; Schrag, J. L. *Trans. Soc. Rheol.* **1962**, *6*, 325.
(5) Miller, J. W.; Schrag, J. L. *Macromolecules* **1975**, *8*, 361.
(6) Soli, A. L.; Schrag, J. L. *Macromolecules* **1979**, *12*, 1159.
(7) Minnick, M. G.; Schrag, J. L. *Macromolecules* **1980**, *13*, 1690.
(8) Lodge, T. P.; Miller, J. W.; Schrag, J. L. *J. Polym. Sci., Polym. Phys. Ed.* **1982**, *20*, 1409.
(9) Lodge, T. P.; Schrag, J. L. *Macromolecules* **1982**, *15*, 1376.
(10) Muthukumar, M.; Freed, K. F. *Macromolecules* **1978**, *11*, 843.
(11) Ferry, J. D. "Viscoelastic Properties of Polymers"; Wiley-Interscience: New York, 1980.
(12) Osaki, K. *Adv. Polym. Sci.* **1973**, *12*, 1.
(13) Brueggeman, B. G.; Minnick, M. G.; Schrag, J. L. *Macromolecules* **1978**, *11*, 119.
(14) Perico, A. *J. Polym. Sci., Polym. Phys. Ed.* **1980**, *18*, 161.
(15) Fetters, L. H.; McIntyre, D., private communication.
(16) Fetters, L. H.; McIntyre, D. *Polymer* **1978**, *19*, 463.
(17) Lodge, T. P. Ph.D. Thesis, University of Wisconsin, 1980.
(18) Riande, E.; Markovitz, H.; Plazek, D. J.; Raghupathi, N. *J. Polym. Sci., Polym. Symp.* **1975**, *No. 50*, 405. D. J. Plazek; E. Riande; Markovitz, H.; Raghupathi, N. *J. Polym. Sci., Polym. Phys. Ed.* **1979**, *17*, 2189.
(19) Miller, J. W. Ph.D. Thesis, University of Wisconsin, 1979.
(20) Schrag, J. L. Ph.D. Thesis, Oklahoma State University, 1967.
(21) Soli, A. L. Ph.D. Thesis, University of Wisconsin, 1978.
(22) Rouse, P. E., Jr. *J. Chem. Phys.* **1953**, *21*, 1272.
(23) Zimm, B. H. *J. Chem. Phys.* **1956**, *24*, 269.
(24) Kuhn, W. *Kolloid Z.* **1934**, *68*, 2.
(25) Kuhn, W.; Grun, F. *Kolloid Z.* **1942**, *101*, 248.
(26) Tsvetkov, V. N. *Polym. Rev.* **1966**, *6*, Chapter XIV.
(27) Gent, A. N. *Macromolecules* **1969**, *2*, 263.
(28) Peterlin, A. *Polym. Lett.* **1967**, *5*, 113.
(29) Peterlin, A. *J. Polym. Sci., Part A-2* **1967**, *5*, 179.
(30) Thurston, G. B.; Peterlin, A. *J. Chem. Phys.* **1967**, *46*, 4881.
(31) Massa, D. J. Ph.D. Thesis, University of Wisconsin, 1970.
(32) Frisman, E. V.; Dadivanian, A. K. *J. Polym. Sci., Part C* **1967**, *16*, 1001.
(33) Tsvetkov, V. N.; Grishchenko, A. E. *J. Polym. Sci., Part C* **1968**, *16*, 3195.
(34) Janeschitz-Kriegl, H. *Adv. Polym. Sci.* **1969**, *6*, 169.
(35) Jones, A. A.; Bisceglia, M. *Macromolecules* **1979**, *62*, 1136.
(36) Yee, A. F.; Smith, S. A. *Macromolecules* **1981**, *14*, 54.
(37) Inglefield, P. T.; Jones, A. A.; Lubianez, R. P.; O'Gara, J. F. *Macromolecules* **1981**, *14*, 288.
(38) Steger, T. R.; Schaefer, J.; Stejskal, E. O.; McKay, R. A. *Macromolecules* **1980**, *13*, 1273.
(39) Champion, J. V.; Desson, R. A.; Meeten, G. H. *Polymer* **1974**, *15*, 301.
(40) Tsvetkov, V. N. *J. Polym. Sci.* **1957**, *23*, 151.
(41) Copic, M. *J. Chem. Phys.* **1957**, *26*, 1382.
(42) Koyama, R. *J. Phys. Soc. Jpn.* **1961**, *16*, 1366.
(43) Koyama, R. *J. Phys. Soc. Jpn.* **1964**, *19*, 1709.
(44) Fortelny, I. *J. Polym. Sci., Polym. Phys. Ed.* **1974**, *12*, 2319.
(45) Minnick, M. G. Ph.D. Thesis, University of Wisconsin, 1980.
(46) Sadron, C. *J. Phys. Radium* **1936**, *9*, 381.
(47) Kovar, J.; Fortelny, I.; Bohdanecky, M. *Collect. Czech. Chem. Commun.* **1973**, *38*, 848.
(48) Gent, A. N.; Kuan, T. H. *J. Polym. Sci., Part A-2* **1971**, *9*, 927.
(49) Tonelli, A. E. *Macromolecules* **1973**, *6*, 682.
(50) Rudd, J. F.; Gurnee, E. F. *J. Appl. Phys.* **1957**, *28*, 1096.
(51) Andrews, R. D.; Rudd, J. F. *J. Appl. Phys.* **1957**, *28*, 1091.
(52) Andrews, R. D.; Kazama, Y. *J. Appl. Phys.* **1968**, *39*, 4891.
(53) Kawata, K. *J. Polym. Sci.* **1956**, *19*, 359.
(54) Rudd, J. F.; Andrews, R. D. *J. Appl. Phys.* **1960**, *31*, 818.
(55) Peterlin, A. *Polym. Prepr., Am. Chem. Soc., Div. Polym. Chem.* **1981**, *22*, 114.
(56) Harris, R. A.; Hearst, J. E. *J. Chem. Phys.* **1966**, *44*, 2595.
(57) Hearst, J. E.; Harris, R. A. *J. Chem. Phys.* **1966**, *45*, 3106.
(58) Cerf, R. *J. Phys. Radium* **1958**, *19*, 122.
(59) Cerf, R. *Adv. Polym. Sci.* **1959**, *1*, 382.
(60) Peterlin, A. *Kolloid Z.* **1966**, *209*, 181.
(61) Fixman, M.; Evans, G. T., private communication.
(62) Adler, R. S.; Freed, K. F. *Macromolecules* **1978**, *11*, 1058.

Influence of Pendant Chains on the Loss Modulus of Model Networks

Miguel A. Bibbó and Enrique M. Vallés*

Planta Piloto de Ingeniería Química, UNS-CONICET, Bahía Blanca 8000, Argentina.
Received August 16, 1983

ABSTRACT: The progress of the loss component of the shear modulus, G'', of a model silicone network has been studied during the cross-linking reaction. It has been observed that G'' increases steadily after the gel point until a maximum value is reached. Then G'' decreases up to a final definite value when the reaction is completed. By a recursive technique, the evolution of the molecular structure of the network with the extent of the reaction was calculated and associated with G'', leading to the conclusion that pendant chains contribute significantly to the loss modulus of an amorphous rubbery material.

Introduction

The study of model rubber networks has been developed extensively during the last years in order to investigate the influence of several structural characteristics on the mechanical properties of these materials. Most of the past research has been focused on the quantitative verification of the theory of rubber elasticity. Several of these studies have been done with poly(dimethylsiloxane) networks[1-8] including some of our own work in which we have looked to the evolution ot the elastic modulus with the extent of the cross-linking reaction.

While working with this chemical system, we have observed that the loss modulus increases steadily after the gel point until a maximum value is reached at a certain extent of reaction. Then G'' decreases up to the completion of the curing process. The same kind of behavior has been observed with networks of different chemical structure like urethanes[9] and epoxies.[10]

In this work we look for a molecular justification of this behavior, studying several silicone networks and simultaneously calculating the evolution of the molecular structure by means of a recursive approach originally proposed by Macosko and Miller.[11,12]

Experimental Section

The model silicone network system that was used for this work

0024-9297/84/2217-0360$01.50/0

Table I
Reactant Characterization

reactant	GPC	titration	IR	purity
Vi-PDMS (B_2,11)	M_n = 11 700 M_w = 23 500	M_n = 11 200	M_n = 10 800	96.9%, 3.1% cyclics by GPC
Vi-PDMS (B_2,21)	M_n = 19 700 M_w = 44 000	M_n = 21 800	M_n = 21 000	97.1%, 2.9% cyclics by GPC
trifunctional cross-linker A_3, $(HSi(CH_3)_2O)_3SiPh$[a]				99% by GC
catalyst, *cis*-$(Pt((C_2H_5)_2S)_2Cl_2)$[b]				

[a] Molecular weight = 330. [b] Catalyst was prepared following the procedure described by G. B. Kauffman and D. O. Cowan.[17]

has been thoroughly described in previous publications.[13] It consists of long molecules of end-vinyl-substituted poly(dimethylsiloxane) and a three-functional silane cross-linker.

Two different lengths of the vinyl-terminated PDMS were used. Their average molecular weights were determined by gel permeation chromatography on a Waters ALC 244 GPL, by end-group analysis, with mercuric acetate,[14] and by infrared spectroscopy on a Pye Unicam SP 4000 spectrometer. The results from this characterization are shown in Table I together with a description of the other reactants used in the cross-linking reaction. The polyfunctional silane was distilled several times up to a purity of at least 99% as verified by a Varian 370 GC using a silicone SE-30-OV-1 column.

The reactants were mixed with a mechanical stirrer and degassed under vacuum to eliminate bubbles. Parts of the reacting mixture were placed simultaneously in a thermostatted cell of an IR spectrometer to follow the kinetics of the cross-linking reaction and between the plates of a Rheometrics mechanical spectrometer to follow the changes in the loss modulus with time. The samples in both instruments were kept at the same temperature, usually 35 °C, up to complete reaction.

After curing, each of the samples was placed in a Sohxlet extractor with toluene to verify if the reaction was completed. It was found that this was the case except for the samples with defect of cross-linker, $r = 0.71$, in which the final extent of reaction was estimated to be $p = 0.96$ by using eq 2.

The kinetics were measured by looking at the decay of the SiH peak at 2134 cm^{-1}. The loss shear modulus was monitored by polymerizing the reactants in the eccentric rotating disks (ERD) mode or in the cone and plate fixture with sinusoidal oscillations. The thickness of the samples in the ERD was varied between 1 and 3 mm, and the maximum deformation applied was 10%. All the experiments were performed at a frequency of 1 rad/s except for a few samples that were tested at 10 and 100 rad/s to look for the effect of the frequency on G''. No difference was observed between the experimental results obtained from the two rotational geometries used in this study.

Theory

To be able to relate the changes of the physical properties of the reacting mixture with the development of the macromolecular structure during the nonlinear polymerization, it is necessary to calculate general relations for different molecular parameters as a function of the extent of the cross-linking reaction and the initial conditions of the reacting media. After the gel point the reacting mixture is composed of three different kinds of chain elements as shown in Figure 1. The first type of chains are the so-called "elastic chains", which are those jointed by both ends to the infinite gel structure. The second type of chains are the "pendant" ones, which are joined by only one end to the gel. Finally we have the "soluble" or "extractable" chains, which are not attached to the gel. Using a recursive approach and assuming equal reactivity of the functional groups and absence of intramolecular reaction we have developed[15] the following expressions for the weight fraction of pendant chains in a network, W_p, obtained by stepwise copolymerization between a tri-

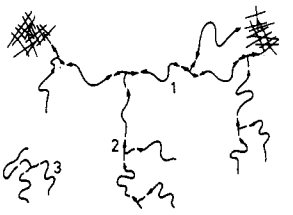

Figure 1. State of the network at intermediate extent of reaction for trifunctional polymerization. Arrows indicate chain ends in the gel direction. (1) Elastic chain; (2) pendant chain; (3) soluble material.

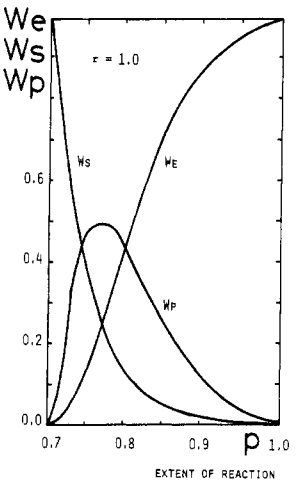

Figure 2. Changes in the weight fraction of elastic, W_e, pendant, W_p, and soluble material, W_s, with extent of reaction, p, for a stoichiometrically balanced mixture of the silicone network used in the experiments.

functional cross-linker, A_3, and a bifunctional prepolymer, B_2, like the PDMS chains of our system.

$$W_p = W_{B_2}\{2[1 - rp + rp\alpha^2][rp + rp\alpha^2]\} + (1 - W_{B_2})\{\alpha(1 + \alpha - 2\alpha^2)\} \quad (1)$$

W_{B_2} = weight fraction of B's in starting mixture

$$\alpha = (1 - rp^2)/rp^2$$

Here p is the extent of the reaction for the A groups and r is the initial stoichiometric imbalance of the reactants; that is, $r = [A]_0/[B]_0$, where $[A]_0$ and $[B]_0$ are the initial concentrations of the functional groups that participate in the reaction. Figure 2 shows how W_p changes with p for a stoichiometrically balanced reaction, together with the evolution of the fraction of elastic material, W_e, and the fraction of soluble material, W_s. These parameters are calculated in a similar way as W_p, giving the following results for a trifunctional cross-linker.

$$W_s = W_{B_2}(1 - rp + rp\alpha^2)^2 + (1 - W_{B_2})\alpha^3 \quad (2)$$

$$W_e = 1 - W_p - W_s \quad (3)$$

Table II
Experimental Data from the Different Networks at W = 1 rad/s

expt	r	M_n of B_2	G'' max, dyn/cm^2	W_p max[a]	p for max G'' exptl	p for max W_p theor[a]
1	1.0924	10 800	30 000	0.5	0.77	0.753
2	0.9247	10 800	27 000	0.5	0.82	0.823
3	0.9858	10 800	18 900	0.5	0.80	0.797
4	0.9863	10 800	16 800	0.5	0.80	0.797
5	0.9783	21 000	44 000	0.5	0.81	0.800
6	0.7115	10 800	10 600	0.5	0.96	0.960
7	0.7103	10 800	10 900	0.5	0.97	0.960
8	0.7112	21 000	23 800	0.5	0.95	0.960
9	0.7102	21 000	25 700	0.5	0.95	0.960
10	1.2347	21 000	60 200	0.5	0.72	0.702
11	1.1849	21 000	59 000	0.5	0.72	0.718
12	1.1923	21 000	45 000	0.5	0.72	0.714

[a] Using eq 1.

At the gel point, all the reacting molecules belong to the soluble fraction, and as the reaction goes on, this fraction decays rapidly to zero. At completion of the curing all the initially reactive molecules are attached to the network and belong to elastic chains joined by both ends to the infinite structure. For this reason the fraction of elastic chains increases steadily from zero to one in the same interval. The relative amount of pendant chains increases from the gel point up to a maximum at $p = 0.79$ in which 50% of the reacting material belongs to this fraction and then decays up to zero at $p = 1.00$.

The extent of reaction at which W_p reaches its highest value and the amount of pendant material that remains in the network at the end of the reaction depends on r. Figure 3 shows a three-dimensional picture of the change of W_p with r and p for all the possible initial imbalances that will end in a network structure with a trifunctional cross-linker, that is $0.50 \leq r \leq 2.00$. The full line curves on the surface correspond to the growth of W_p with p for different initial stoichiometries. The projection of the surface on the $W_p = 0$ plane represents the domain of all the possible combinations of p and r consistent with the existence of a gel structure. The boundary line closest to $p = 0$ indicates the minimum extent of reaction needed for gelation. The two other boundary lines point out the completion of the reaction that is obviously equal to $p = 1.00$ for $r \leq 1.00$ and $p = 1/r$ for $r > 1$.

At moderate imbalances, $0.70 < r < 1.65$, W_p reaches a maximum before the end of the reaction. When the imbalances are important, $1.65 < r < 2.00$ and $0.50 < r < 0.70$, the fraction of pendant material increases steadily during the whole curing process.

The region of moderate imbalances is the one that is important from a practical point of view since most networks are reacted close to $r = 1.0$. It is interesting to indicate that in this zone the maximum value for the pendant fraction is always equal to $W_p = 0.50$; that is, when W_p peaks, half of reacting media is composed of pendant chains.

Another parameter of importance is the average molecular weight of pendant chains since this gives a way to estimate the average size of these chains. The weight average molecular weight, $M_{w,p}$, has been calculated in a previous publication, in which we show that this parameter decreases continuously with p from the gel point to the completion of the reaction.[16] The equation that corresponds to a trifunctional system is

$$M_{w,p} = a'_d E(W_{A_3,d}) + a'_r E(W_{A_3,r}) + b'_d E(W_{B_2,d}) \quad (4)$$

where a'_d is the weight fraction of A_3 in the pendant material, b'_d is the weight fraction of B_2 in the pendant material, $a'_r = 1 - a'_d - b'_d$, $E(W_{A_3,d})$ is the expected weight from a cross-linker A_3 group on a dangling chain, $E(W_{A_3,r})$ is the expected weight from a crosslinker A_3 group on the function that joins the pendant chain to the gel, and $E(W_{B_2,d})$ is the expected weight from a bifunctional B_2 group on a dangling chain.

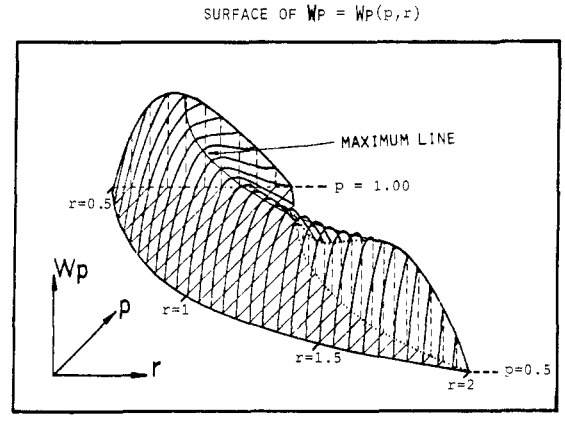

Figure 3. Calculated fraction of pendant material, W_p, as a function of the extent of reaction, p, and stoichiometric imbalance r. W_p reaches a maximum during the cross-linking reaction at moderate imbalances $0.70 < r < 1.65$.

Explicit expressions for these three expected weights as function of the known variables r and p are given in ref 16.

Results and Discussion

From the kinetic measurements obtained from the infrared spectrometer and the rheological observations of G'' vs. time, the loss modulus was determined as a function of the extent of reaction. The weight fraction of pendant material and the weight average molecular weight of the dangling chains were calculated with eq 1 and 4. It was known from previous work that the silicone system used in the experiments was almost ideal since the chemical groups that participate in the reaction are equally reactive, and no significant amount of intramolecular reactions was detected.[13] This was done by measuring accurately the onset of gelation, which showed no delay with the theoretical gel point.

Twelve runs were performed in this study with different initial stoichiometries and with two distinct molecular weights of the bifunctional PDMS prepolymer. In Table II we list the principal characteristics of each run, together with extent of the reaction at which the maximum value of G'' was measured. In Figures 4, 5, and 6 we show the evolution of the loss modulus with p for nine runs that

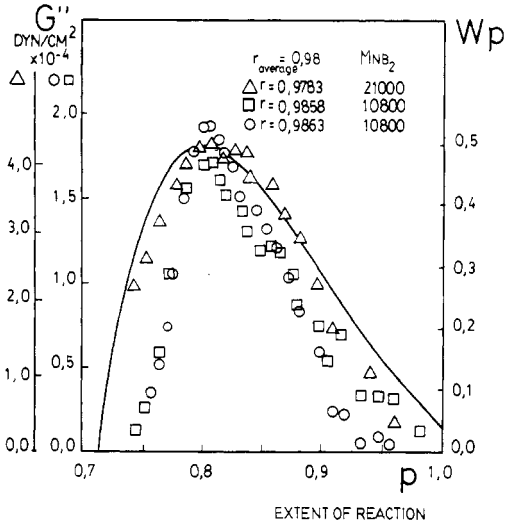

Figure 4. Experimental results from runs number 3 (□), 4 (○), and 5 (△). Single points correspond to G'' measurements. Full line shows the calculated change of W_p from eq 1. The scales of the experimental data have been chosen to get the maximum G'' value at the same level for all the runs.

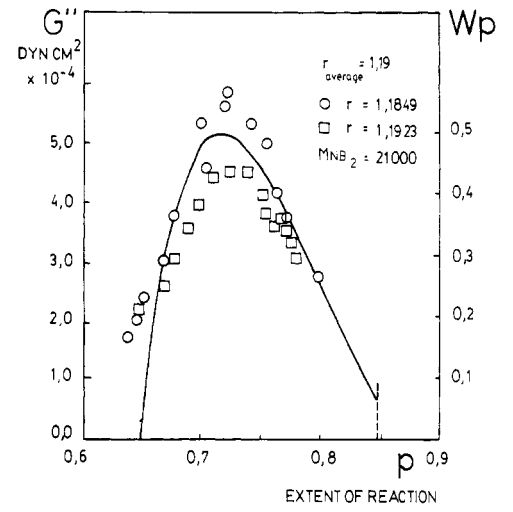

Figure 5. Experimental results from runs number 11 (○) and 12 (□). See Figure 4.

correspond to an almost balanced stoichiometry and a reaction with excess and defect of cross-linker, respectively. The points show the number of readings of G'' for each run.

The loss modulus was not measured continuously to reduce to a minimum the disturbances in the reacting media. On repeated runs with dissimilar spacings in time for the loss modulus measurements, no difference was observed for the readings of G''. This means that the structure of the network was not affected by the discontinuous stress induced on the sample by the rheometer. The three graphs also show the calculated curves for W_p vs. p at imbalances of r = 0.99, 0.71, and 1.19, and the experimental results for G'' in each case. The scales of the abscissas for the loss modulus have been selected in such a way that the maximum value of G'' is at the same level as the maximum value for the fraction of pendant material, which is W_p = 0.50 in the three cases. As it may be seen there is a great similarity between the shapes of the theoretical curves for W_p and the experimental results for G''. It is also appreciable that the coincidence is better when the prepolymer of higher molecular weight is used. This may be attributed to the fact that with this prepolymer the level of the signal in the rheometer for the measurement of G'' is considerably higher and the accurancy of the readings in the regions of low modulus is improved significantly. The extent of the reaction for the maximum loss in all the runs agrees within experimental error with the extent of reaction at which the fraction of pendant material peaks. Figure 7 highlights this coincidence on a p vs. r plot for the 12 runs. The dotted line on the left corresponds to the gelation line and the other on the right to the extent of reaction of A groups at complete reaction. The full line indicates the calculated extent of reaction for the maximum fraction of pendant material. The dots show the experimental extent of reaction at the moment of maximum loss for all the runs as indicated in Table II.

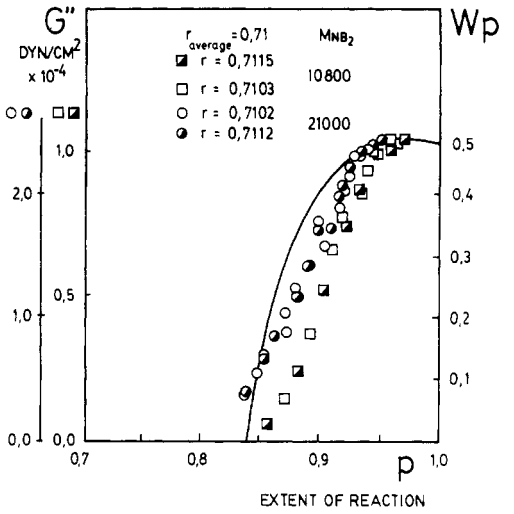

Figure 6. Experimental results from runs number 6 (◪), 7 (□), 8 (◐), and 9 (○). See Figure 4.

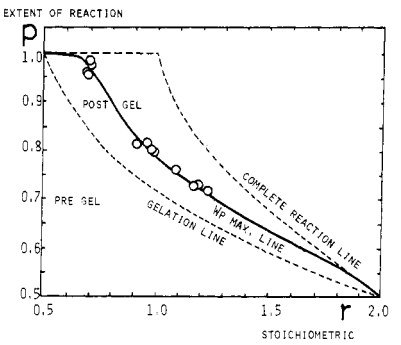

Figure 7. Agreement between maximum loss modulus for all the runs and calculated maximum fraction of pendant material in the network.

From these results we conclude that there is a very close relationship between the amount of pendant material and the loss modulus, the dangling chains being one of the more important structural factors that contribute to the energy dissipation of a rubber during a dynamic deformation experiment at low frequency. We think that this phenomenon can be explained qualitatively by looking to the structural characteristics of the pendant chains. As these elements are joined to the gel by one of their ends, when an external strain is applied to the network the chains must follow the deformation on the junctions. At the beginning of the deformation the dangling chains will be strained very similary to the elastic chains. But, as all the other ends of the pendant chains are free to move in any direction, they will immediately begin to reaccomodate toward a higher entropic configuration. If the strain is then released or inverted, like in a dynamic test, the elastic chains will restore most of the energy spent on their deformation. On the other hand, the dangling chains will restore only part

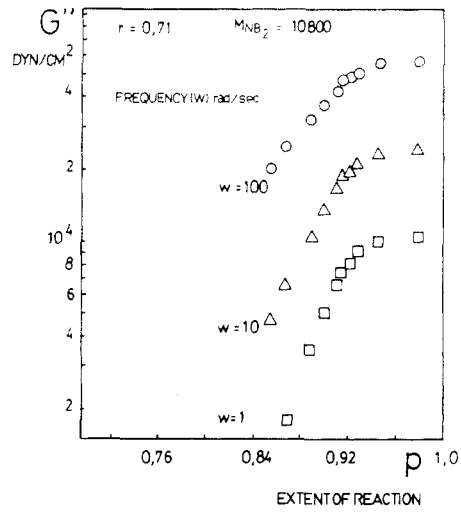

Figure 8. Frequency dependence of the loss modulus curves during the cross-linking reaction.

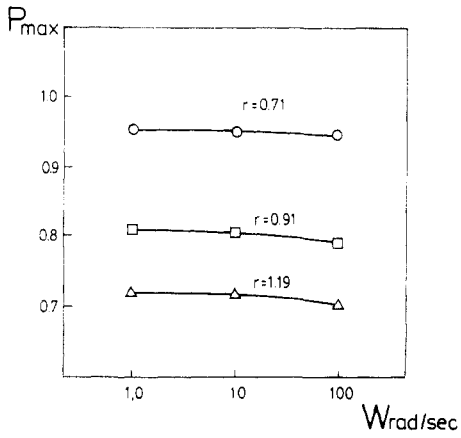

Figure 9. Extent of reaction at maximum G'' for each system as a function of frequency.

or none of the energy, depending on the frequency of the test. In an extreme situation, if the chains have enough time to relax to a new equilibrium configuration, all the energy spent on the deformation of the dangling chains will be dissipated. Moreover, it will be necessary to spend more energy while the network is returning to its original shape since at that time the dangling chains will be deformed once more to a new strained position and then the reaccomodation process will take place again. It is clear from this picture that the pendant chains have much more potential for energy dissipation than the elastic chains or the sol fraction. At higher frequencies the contribution to the loss modulus of each part of the structure of the network is more complicated. Figure 8 shows how frequency affects the evolution of the loss modulus with the extent of reaction for imbalances of $r = 0.71$. As it may be appreciated, besides the expected increase on the absolute value of G'', there is a tendency to obtain a wider and flatter maximum zone and to displace slightly the maximum toward a lower extent of reaction. This is also observed for the other imbalances as we show in Figure 9, in which the displacement of the maximum in G'' with frequency is reported. We believe that these displacements reflect the contribution of the weak gel structure and the sol fraction to the loss modulus. The results reported here cover only a narrow portion of the time spectrum. Unfortunately it was not possible in our work to obtain more information at lower frequencies. Measurements at $\omega <$ 1.0 rad/s imply low signals and long reading times, which

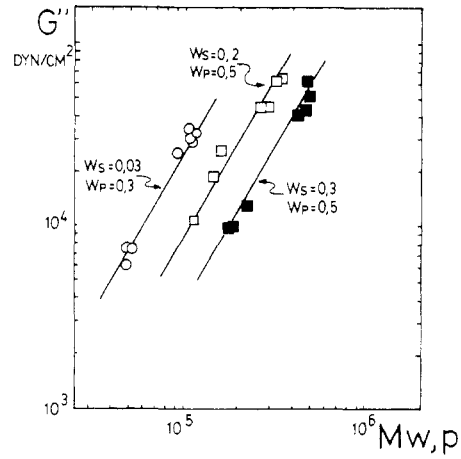

Figure 10. Relation between loss modulus and weight average molecular weight of the pendant chains. Circles correspond to measurements for G'' on samples with a weight fraction of pendant chains $W_p = 0.30$ and a low content of soluble material $W_s = 0.03$, squares to runs for $W_p = 0.5$ and $W_s = 0.2$, and solid squares to $W_p = 0.5$ and $W_s = 0.3$.

introduce uncertainties when one is dealing with a reactive system.

This qualitative description does not take into account any information concerning the size and shape of the pendant chains. To do that we have recently developed several calculations to estimate the average structural characteristics of the pendant chains. Using some of these calculations we show in Figure 10 the dependence of the loss modulus with the weight average molecular weight of the pendant chains. This has been done by using eq 1, 2, and 4 and looking for values of G'' and $M_{w,p}$ on the different runs at equivalent W_p and W_s.

The experimental information obtained with the two prepolymers used in this work is not enough to cover a wide region of molecular weight, but it is clear that G'' increases with $M_{w,p}$ and decays with dilution. The slope of all the straight lines in the log–log plot is approximately 1.5. More experiments are needed with at least two other average lengths of the prepolymer to look for more detailed information on the dependence of G'' with average molecular weight and degree of branching of the pendant material. This work is in progress in our laboratory and will be the subject of a future publication.

Acknowledgment. We express our gratitude to the National Research Council Argentina (CONICET) which supported this work and to Dr. Neal Langley from the Dow Corning Corporation that kindly supplied the PDMS reactants.

References and Notes

(1) E. M. Vallés and C. W. Macosko, *Rubber Chem. Technol.*, **49**, 132 (1976).
(2) J. E. Mark and J. L. Sullivan, *J. Chem. Phys.*, **66**, 1006 (1977).
(3) M. A. Llorente and J. E. Mark, *J. Chem. Phys.*, **71**, 682 (1979).
(4) E. M. Vallés and C. W. Macosko, *Macromolecules*, **12**, 673 (1979).
(5) M. A. Llorente and J. E. Mark, *Macromolecules*, **13**, 681 (1980).
(6) K. P. Meyers, Ph.D. Thesis, Department of Chemical Engineering, Massachusetts Institute of Technology, 1980.
(7) M. Gottlieb, C. W. Macosko, G. S. Benjamin, K. O. Meyers, and E. W. Merrill, *Macromolecules*, **14**, 1039 (1981).
(8) E. J. Rost, Masters Thesis, Universidad Nacional del Sur (UNS), 1982.
(9) F. Mussatti, Ph.D. Thesis, Department of Chemical Engineering, University of Minnesota, 1974.
(10) R. L. Hassel, *Ind. Res. Dev.*, **20**, 160 (1978).
(11) D. R. Miller and C. W. Macosko, *Macromolecules*, **9**, 199 (1976).

(12) D. R. Miller and C. W. Macosko, *Macromolecules*, **9**, 206 (1976).
(13) E. M. Vallés and C. W. Macosko, *Macromolecules*, **12**, 571 (1979).
(14) R. C. Smith, "Analysis of Silicone", Wiley, New York, 1974.
(15) D. R. Miller, E. M. Vallés, and C. W. Macosko, *Polym. Eng. Sci.* **19**, 272 (1979).
(16) M. A. Bibbó and E. M. Vallés, *Macromolecules*, **15**, 1293, (1982).
(17) G. B. Kauffman and D. O. Cowan, *Inorg. Synth.* **6**, 214 (1960).

Correlation of Liquid-State Compressibility and Bulk Modulus with Cross-Sectional Area per Polymer Chain

Raymond F. Boyer* and Robert L. Miller

Michigan Molecular Institute, Midland, Michigan 48640. *Received January 24, 1983*

ABSTRACT: Liquid-state compressibilities, $\kappa = -(1/V_0)(\partial V/\partial P)$, determined at $P \rightarrow 0$ and at the liquid–liquid transition (relaxation), $T_{ll} \sim 1.2T_g$ (K), increase as $A^{0.54}$, where A is the cross-sectional area per polymer chain calculated at 20 °C from X-ray lattice parameters. κ increases from 3.8×10^{-5} to 7.4×10^{-5} bar^{-1} as A increases from 0.280 to 0.934 nm^2. Since $A^{0.5}$ is an average interchain distance, κ thus increases linearly the further apart are the chains. The bulk modulus, $\bar{K}$, and the Tait equation parameter, b, both in bars, decrease as $A^{-0.52}$, again at $P \rightarrow 0$ and at T_{ll}. Correlations of κ, $\bar{K}$, and b with A at $T_g + 100$ K were inferior to those at T_{ll}, with smaller correlation coefficients and larger standard errors. T_{ll} thus appears to be a useful liquid-state reference temperature. Corrections for thermal expansion and ratios of amorphous density to crystalline density were not made. κ values for linear and branched PE's and for a mixed-isomer PBD did not fit the correlation, with κ being high. Values of κ for the glassy state at $T \rightarrow T_g$ did not correlate with A. Ability to detect liquid-state transitions from isothermal V–P data should increase with area per chain because of enhanced compressibility. This is demonstrated for PS.

Introduction

We have been interested for some time in empirical or semiempirical correlations of selected physical properties of polymers with cross-sectional area, A, of polymer chains. Properties studied thus far are the Mooney–Rivlin C_2 constant,[1,2] the chain entanglement parameter N_c,[3,4] surface fold energy σ_e,[5] the chain stiffness parameter σ,[6] and the critical tensile strength.[7]

Areas are calculated from X-ray lattice parameters of crystalline polymers or by several indirect methods for amorphous polymers and copolymers.[2,4] In addition to values of A that have been published,[2,4] one of us maintains an extensive tabulation of A values.[8] As explained earlier,[2] values of A are valid at 20 °C and are assumed to hold for amorphous polymers even though derived for crystalline polymers. We justified this practice since the ratio of amorphous density to crystalline density is about 0.9 for many polymers.[2] Also, we do not correct herein for effects of thermal expansion on A.

We have examined correlations of still other polymer properties with A. These are as yet not formalized into a finished product. In the course of such studies we became aware that the liquid-state isothermal compressibility, κ, increases with area, where κ at $P \rightarrow 0$ is defined as

$$\kappa = -(1/V_0)(\partial V/\partial P) \quad (1)$$

with V being the specific volume in cm^3 g^{-1} at the pressure in bars (P) and V_0 the specific volume at zero pressure, giving κ the dimension of bars^{-1}. κ is a function of both T and P. It increases with T and decreases with P at constant T. Both of these facts complicated our early attempts at correlation of κ with A. We arbitrarily chose values of κ at $T_g + 100$ °C and $P = 1$ bar in our original correlations but this choice for a reference temperature was not satisfactory. κ did increase with log A but there was considerable scatter.

The problem is analogous to that with the monomeric friction coefficient, Ξ_0, calculated from melt viscosity data. Ξ_0 is also a function of T. Ferry[9] has presented tabulated values of Ξ_0 at several different temperatures, i.e., 298 K, $T_g + 100$ K, etc.

Procedural Details

We have elected in what follows to calculate κ at T (K) $= kT_g$ (K), where k is a constant slightly greater than unity. The evolution of this choice is as follows.

κ is commonly obtained from isothermal V–P data as eq 1 suggests. One of us has been analyzing published V–P data[10-13] and isobaric V–T data at $P \leq 600$ bar,[14] as a means of locating secondary liquid-state transition (relaxation) temperatures, notably the liquid–liquid events designated by us as T_{ll} and T_{ll}'.[15-17] (See Appendix for terminology.) Pertinent to the present study was the determination of the Tait equation parameter, b, in bars, as a function of temperature.[12] Specifically, we calculated b as $P \rightarrow 0$ and labeled this value as b^*.

We have discussed elsewhere[10] the approximate relationship

$$\kappa \cong (C/b)(1 - P/b) \quad (2)$$

valid for $P/b < 0.4$. C is a constant, usually given as 0.0894 unless noted otherwise.[10] One obtains κ at $P \rightarrow 0$ as C/b^*. We showed[12] that b^* decreased linearly with T from $T_g < T < T_{ll}$ and again linearly with a smaller slope above T_{ll}. κ will therefore increase with T somewhat curvilinearly but with a distinct slope change at T_{ll}. It was proposed tentatively[12] that T_{ll} be considered a liquid-state reference temperature. Plots of b^* vs. T/T_{ll} for many of the polymers in Table I are shifted horizontally to coincide at $T/T_{ll} = 1$ but are separated vertically by structure. (See Figures 6 and 7 of ref 12.)

Slopes, db^*/dT, below and above T_{ll}, given in Table III of ref 12, are different for each polymer. This study[12] convinced us that T_{ll} might be considered a reference temperature characteristic of the liquid state. Since T_{ll} (K)$/T_g$ (K) $\sim 1.20 \pm 0.05$ for most polymers with $\bar{M}_n$ above the oligomeric range,[12-17] one may prefer to consider our

0024-9297/84/2217-0365$01.50/0